

Reconfigurable and Programmable Metamaterials

Subjects: Electrochemistry

Contributor: Lei Chen

As an emerging research product in the 21st century, or a new type of artificial composite functional material, metamaterials are subwavelength artificial composite structural materials, whose unit size is generally less than half of the working wavelength.

Keywords: metamaterial ; metasurface ; electromagnetic manipulation ; tunable metasurfaces ; active programmable metasurfaces ; intelligent metasurfaces

1. Introduction

The concept of electromagnetic (EM) metamaterials originated from a Russian paper published by Veselago ^[1], a scientist of the former Soviet Union, in 1967. Later, it was translated into English and published in 1968, and “metamaterials” gradually became known to the world. Veselago also proposed left-handed materials, which have negative dielectric constants and magnetic conductivity ^{[2][3][4]}. Although this breakthrough concept subverted people’s cognition of traditional electromagnetic materials, the theory received little attention at that time because such double-negative materials could not be obtained in nature, and it was difficult to be verified by experiments. Until 1996, Pendry proposed a structure ^[5] in which the metal wires were arranged periodically according to certain rules, and finally the material with negative dielectric constants was obtained. By adjusting the period and the radius of the metal wires, the plasma frequency can be reduced to the microwave range. Later, in 1999, he further proposed to nest the two open copper rings inside and outside ^[6], which was the split-ring resonator (SSR). When working near the resonant frequency of the SRR ring, it can exhibit negative magnetic conductivity. Based on these theories, in 2001, D. R. Smith et al. combined the two structures and designed them to make the two negative frequency bands coincide ^[7], producing the first artificial electromagnetic metamaterial. Generally, with three-dimensional structure, electromagnetic metamaterials have unique physical properties that traditional materials do not have, such as inverse Cherenkov radiation effect, negative refractive index ^{[8][9][10][11]}, lens ^{[12][13][14][15]}, cloaking ^{[16][17][18][19][20][21]}, illusion devices ^{[22][23]}, and so on. Today, metamaterials have developed into a multi-disciplinary and comprehensive research direction, whose research field is no longer limited to the electromagnetic field, but expanded to acoustics ^[13], thermal science ^[24], quantum mechanics ^[25], informatics ^[26], biomedical ^{[27][28]}, and other disciplines, forming an extremely wide coverage and far-reaching important discipline. Metamaterials provide a wide space for people to manipulate electromagnetic waves ^[13] and even acoustic and mechanical waves ^[29] freely with their super freedom of design, and further give rise to new electromagnetic applications such as perfect imaging ^{[30][31]}, holographic imaging ^{[32][33][34][35][36]}, electromagnetic black hole ^[37], metamaterial lenses ^{[12][38][39][40][41]}, and other EM designs with multiple functions ^{[42][43]}.

The initial research work of electromagnetic metamaterials is based on electromagnetic resonant structures in three-dimensional form, which are usually composed of metal and its dielectric structure stacked on top of each other. Such structural design is extremely difficult in actual fabrication, so the structure verification of three-dimensional metamaterials adopts single-layer two-dimensional structure. In addition, the three-dimensional metamaterial structure also has many limitations in terms of material loss and working frequency band. Therefore, how to realize two-dimensional electromagnetic metamaterials, namely electromagnetic metasurface, has gradually become the focus of scientific attention. In 1999, Sievenpiper first proposed a high impedance surface similar to a mushroom-shaped structure ^[44]. This kind of magnetic tape gap structure is considered to be one of the early studies of the electromagnetic metasurface because of its periodic arrangement of subwavelength and effective suppression of specific surface wave patterns. Capasso’s team published a paper in the journal *Science* that proposed “generalized Snell’s law” in 2011 ^[45], which became an important turning point in the history of metasurface research. They used a V-shaped element to achieve reflective control of the geometric phase. By changing the opening angle and rotation angle of the V-shaped arms, the reflective phase can be covered by 360°. Based on this regulation of the abrupt phase of the surface, Capasso’s team showed that both the gradient phase distribution and the rotational phase distribution can be used to deflect the scattered beam and generate the vortex beam, respectively. Thanks to the new methods and ideas provided by the generalized

Snell's law for people to design electromagnetic metasurfaces, a large number of studies on the application of metasurfaces are emerging. With the advantages of excellent electromagnetic control ability, low profile, low loss, and easy processing, two-dimensional metasurface has been the leader in the research of metamaterials in the last ten years, which has stimulated a variety of functions and applications, such as holographic imaging [46][47][48], vortex beam [49][50][51][52][53], ultra-thin invisibility cloak [54], absorbers [55][56][57], Huygens metasurface [58][59], non-magnetic non-reciprocity metasurfaces [60][61][62], and so on.

Most of the early metasurfaces were passive structures. In order to explore and extend the dynamic tunable function of metasurfaces, active and tunable metasurfaces have been proposed successively [63]. Compared with the passive metasurface, the active metasurface usually has the advantages of a wide frequency band, large adjustable range, and low loss, which brings great vitality for the development of the metasurface. Gil's team implemented a frequency-tunable filter by introducing a varactor diode into the open resonant ring [64]. Then, by filling the opening resonant gap with N-type silicon material containing light doping [65], Aloyse controlled the light with metamaterial. Later, some researchers used active devices to achieve tunable electrically controlled metamaterials and tunable magnetically controlled metamaterials [66]. The core idea of the active tunable metasurface is to load active devices on each element, and realize the functions of polarization conversion [67][68], beam scanning [69], multi-beam, and wave absorption [70] while keeping the physical structure of the unit unchanged. Active devices include a varactor diode, triode, sensor, and so on. At present, the regulation methods of the tunable metasurface mainly include mechanical control [71][72][73], electric control [74][75], temperature control [76], and light control [77]. Mechanical control is to manipulate the phase by adjusting the physical size or rotation angle. Additionally, the electronic devices commonly used in electrical control are: PIN diodes, varactor diodes, and MEMS switches. Compared with mechanical control, electric control has lower system complexity, more flexible regulation form, and stronger beam regulation ability. By adopting appropriate regulation mode, the active tunable metasurface can enlarge the manipulation range of the phase and polarization mode of electromagnetic wave in microwave frequency band, and plays an irreplaceable role in realizing arbitrary polarization and arbitrary beam control. At the same time, the combination of metasurface and tunable materials such as graphene can make great contributions to the progress of terahertz technology [78][79], visible light [54][80], and the infrared light field [11][81].

To explore the possible connection between metasurface and digital information, Engheta's team put forward the concept of "digital metamaterial" in 2014 [82] and proposed that the discrete structural design method can be introduced into the design process of metamaterial. However, this concept is still limited to the digitization of equivalent medium parameters, so it is hard to realize, and no follow-up research has been carried out. Meanwhile, Cui Tie Jun proposed a new theory of digital coding programmable metasurface in 2014 [83], opening a new chapter in metasurface research. The core idea of digital coding metamaterials is to introduce digital binary code into the design of metamaterials. Furthermore, digital information is integrated into all aspects of the design of metamaterials [84], such as structure, electromagnetic parameters, and functions. Since then, diverse EM functional designs in passive coding metasurface design has been proposed, such as holography [85][86], full-space control [87], acoustic field modulation [88], optically transparent metasurfaces [89][90], orbital angular momentum (OAM) beams [91], and multi-frequency manipulation [92][93]. However, due to the functional solidification of passive coding metasurface, its application scenarios and practical value are greatly limited [94]. Active programmable coding metamaterials are the inevitable direction of passive structure function extension. So far, plenty of active programmable metasurfaces based on PIN diodes and varactors have emerged, and the coding form has gradually expanded from the programmable phase [95][96] to programmable amplitude [97] and polarization [98][99]. However, active control of programmable metamaterials still requires human intervention to change the control instructions or programs to achieve the switch of different electromagnetic characteristics [100], such as switching different phase coding states, different polarization coding states, etc. Therefore, the intelligent metamaterials will be an important direction in the future development of metamaterials [100][101][102][103].

2. Intelligent Metasurfaces

As an active and controllable form of coding metamaterials, programmable metasurfaces provide a hardware basis for the functional diversity of information metamaterials. A variety of programmable metasurfaces, such as phase, amplitude, and polarization programmable metasurfaces, have been proposed successively, showing the excellent electromagnetic manipulation ability of programmable metamaterials. However, at present, almost all programmable metasurfaces require human participation in the regulation of their electromagnetic characteristics or functions, that is, the operation of the control part needs to be carried out with the help of human subjective judgment and recognition. For intelligent metasurfaces, adaptive intelligent operation must make them have the ability to identify and judge the environmental changes actively [100][101], so as to make autonomous decisions according to certain intelligent algorithms.

For this reason, this work assumed a special application scenario, as shown in **Figure 1 a**. It is supposed that the reflected beam of a metasurface on a dynamic aircraft demands to be aligned adaptively to a satellite in real time for communication. When the aircraft is in different flight directions, the scattering angle of the electromagnetic beam scattered by the smart metasurface needs to be automatically aligned with the satellite in a fixed direction. In this control system, metasurfaces require to have the ability to detect the motion and attitude of the aircraft actively, as well as intelligent algorithms to process the perceptive data and make real-time decisions. Therefore, as depicted in **Figure 1 b**, based on conventional programmable metasurfaces with programmable elements and control links, sensors are further added and a microcontroller unit (MCU) with intelligent feedback algorithm is loaded to form a closed-loop control loop [100]. Sensors on the metasurface can detect some certain characteristics of the metasurface and its environment (for example, spatial attitude, motion state, and temperature). In this control loop, the traditional programmable metasurface FPGA will no longer demand manual control, but directly through the MCU after some analysis and processing for intelligent manipulation. When the sensor detects the angle of aircraft attitude changes, the sensory data directly transmit to the MCU. Additionally, according to the change of attitude angle difference, as well as the set beam function (such as beam gaze communication), the MCU can calculate the required direction deflection quickly and generate a set of corresponding coding sequences of the metasurface. In this way, the complete adaptive closed-loop control is realized. This design idea makes the programmable metasurface possess the ability of intelligent judgment and decision in a real sense and provides a new idea for the intelligent development of the metasurface in the future.

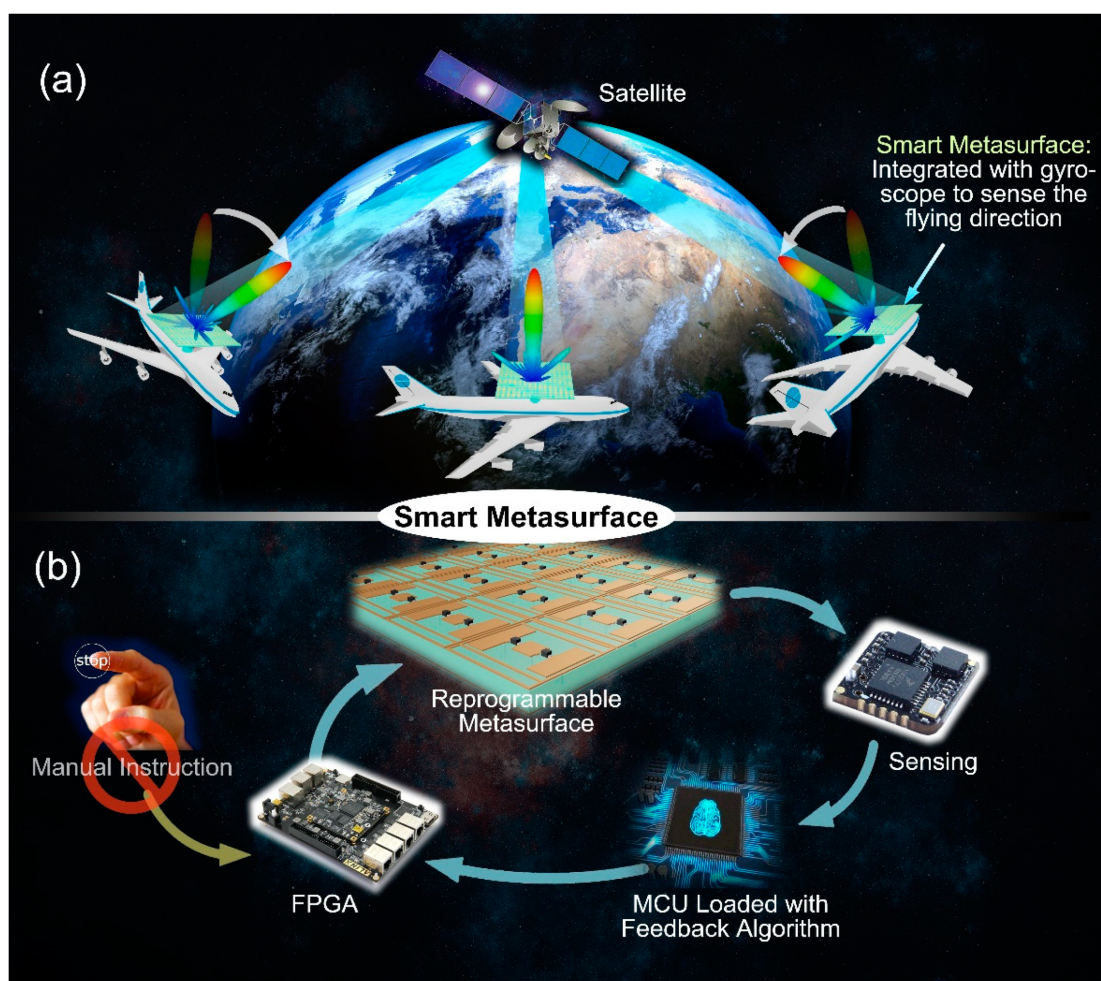


Figure 1. (a) The schematic diagram of the application scenario of metamaterial satellite communication on dynamic aircraft (from Figure 1a of Ref. [100]). (b) Intelligent metasurface control architecture: programmable metamaterials, sensing devices, intelligent feedback algorithms constitute a closed-loop decision loop (from Figure 1b of Ref. [100]). Reproduced with permission from Ref. [100] under a Creative Commons Attribution 4.0 International License. Copyright 2019, Springer Nature.

The intelligent metasurface shown in **Figure 1** integrates sensors by a wire connection. Because the sensing device is separated from the programmable metasurface, and the metasurface cannot complete the sensing function, so the relative integration degree is low. **Figure 2** introduces a dual-polarization programmable metasurface with intelligent sensing function [101], which can detect the polarization direction and energy of incidence wave actively and realize multi-functional intelligent beam manipulation. The metasurface consists of two types of units: the sensing unit and the executing unit. The executive unit is a common programmable metasurface unit, while the sensing unit has two functions of sensing and regulating electromagnetic waves. Under the illumination of different, polarized wave, the sensing units

can obtain a DC voltage reflecting the incidence power level through the receiving circuit. After detecting the voltage, the MCU converts the analog voltage into a digital signal. Then, according to the preset control algorithm, it determines what kind of scattering field control instruction of the metasurface is adopted and transmits the instruction to the FPGA. Finally, the FPGA executes corresponding instructions to manipulate the diode voltage on the metasurface. As shown in **Figure 2 b**, the RF detection circuit module is an important part of the sensing unit, which is composed of a commercial RF detection chip and peripheral circuit. Each sensing unit is equipped with such a group of sensing detection module circuit. At this point, the sensing unit can import the coupling energy of the surface metal patch through the hole to the back microstrip line connected with the RF detection circuit module, so as to realize the corresponding function. **Figure 2 c, d** show the bottom views of the sensing units for the x- and y-polarizations. The microstrip lines of the x-polarization sensing unit are designed along the x-axis, while the microstrip lines of the y-polarization sensing unit extends along the y-axis and enters the detection circuit along the x-axis after a 45° broken line transition. This is designed to minimize the energy loss associated with turning corners. In order to verify the RF power detection performance of the sensing link, the output voltage of the detection circuit under different incidence wave power is tested. **Figure 2 e** shows the test results of the three frequency points of 4.8 GHz, 4.9 GHz and 5.0 GHz. As can be seen from the diagram, when the input power of the horn antenna is greater than about 10 dBm, the output voltage increased obviously from 0.15 V to more than 0.3 V. The results of the dual-beam scattering field in the two polarization directions (x- and y-polarizations) are listed in **Figure 2 f,g**. Two obvious scattering beams, respectively, direct to the x-and y-axes, and this verifies the coding design of double beam deflection.

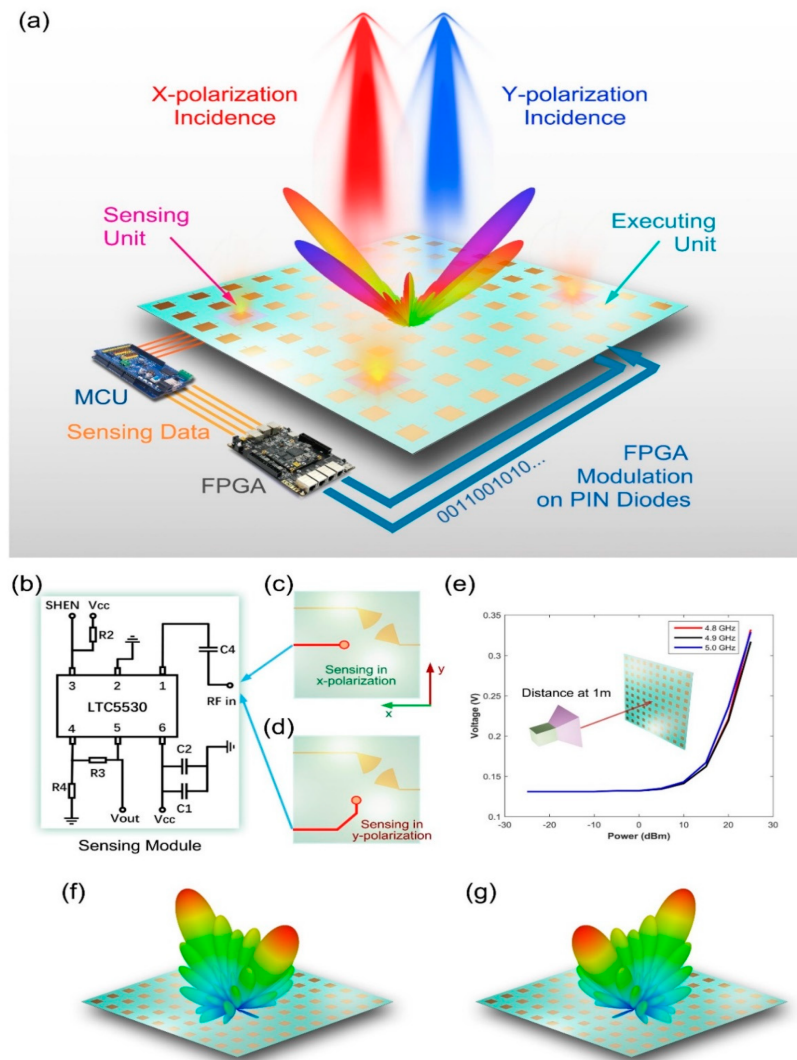


Figure 2. (a) Diagram of a dual-polarization programmable metasurface with intelligent sensing function (from Figure 1 of Ref. [101]). (b) The RF detection circuit module (from Figure 3a of Ref. [101]). (c,d) The bottom views of the sensing units for the x- and y-polarizations (from Figure 3a,c of Ref. [101]). (e) The test results of the three frequency points of 4.8 GHz, 4.9 GHz and 5.0 GHz (from Figure 3d of Ref. [101]). (f,g) The results of the dual-beam scattering field in the two polarization directions (x- and y-polarizations; from Figure 4b,c of Ref. [101]). Reproduced with permission from Ref. [101] under a Creative Commons Attribution 4.0 International License.

3. Conclusions

Looking back at the development trend of electromagnetic manipulation since it first attracted public attention, we can summarize several important stages. The first stage, research on electromagnetic manipulation, initially focused on passive metasurface design. The disadvantage of a passive metasurface is that once the metasurface is prepared, its function is fixed, which limits its application to some extent. Therefore, in order to realize the dynamic operation of electromagnetic waves, the form of electromagnetic manipulation evolves from passive to active tunable metasurface, which is the second stage. The core idea of tunable metasurface is to manipulate the electromagnetic wave without changing the physical structure of the element itself. At present, the regulation forms of the tunable metasurface include mechanical control, temperature control, light control, and so on. Great examples are given to illustrate the design methods of different tunable metasurfaces and how they can achieve flexible manipulation of phase and amplitude responses. In the third stage, with the emergence of the new theory of “digital coding programmable metasurface” a new chapter of metasurface electromagnetic manipulation has been initiated. The key idea of digitally encoding metamaterials is to introduce digital binary code into the design of metasurfaces and utilize the state arrangement of “0” and “1” to manipulate electromagnetic waves. We introduce active programmable metasurfaces based on a varactor, a triode amplifier, and a sensor. By encoding elements with different phases to form different coding sequences, the beam modulation of the scattering field is realized. In the fourth stage, electromagnetic manipulation has stepped into the adaptive and smart age, with the development of self-adaptively intelligent metasurface. Different from previous programmable metasurfaces, which must be controlled by human intervention, the new intelligent metasurface control system will realize autonomous perception, autonomous decision-making, and even adaptive functional control to a certain extent. For the future stage, because the digital coding metasurface needs to be controlled by FPGA to achieve a specific functional design, and the size of the FPGA cannot be ignored in practical application, which will inevitably affect the convenience and integration of the programmable metasurface. Therefore, whether the intelligent programmable metasurface can be separated from the FPGA and realize independent regulation of each element will be the potential direction to promote the development of intelligent metasurfaces.

References

1. Veselago, V.G. Electrodynamics of substances with simultaneously negative and. *Usp. Fiz. Nauk* 1967, 92, 517.
2. Smith, D.R.; Kroll, N. Negative refractive index in left-handed materials. *Phys. Rev. Lett.* 2000, 85, 2933.
3. Houck, A.A.; Brock, J.B.; Chuang, I.L. Experimental observations of a left-handed material that obeys Snell's law. *Phys. Rev. Lett.* 2003, 90, 137401.
4. Garcia, N.; Nieto-Vesperinas, M. Left-handed materials do not make a perfect lens. *Phys. Rev. Lett.* 2002, 88, 207403.
5. Pendry, J.B.; Holden, A.J.; Stewart, W.J.; Youngs, I. Extremely low frequency plasmons in metallic mesostructures. *Phys. Rev. Lett.* 1996, 76, 4773–4776.
6. Pendry, J.B.; Holden, A.J.; Robbins, D.J.; Stewart, W.J. Magnetism from conductors and enhanced nonlinear phenomena. *IEEE Trans. Microw. Theory Tech.* 1999, 47, 2075–2084.
7. Shelby, R.A.; Smith, D.R.; Schultz, S. Experimental verification of a negative index of refraction. *Science* 2001, 292, 77–79.
8. Valentine, J.; Zhang, S.; Zentgraf, T.; Ulin-Avila, E.; Genov, D.A.; Bartal, G.; Zhang, X. Three-dimensional optical metamaterial with a negative refractive index. *Nature* 2008, 455, 376.
9. Veselago, V.G.; Narimanov, E.E. The left hand of brightness: Past, present and future of negative index materials. *Nat. Mater.* 2006, 5, 759–762.
10. Xiao, S.; Drachev, V.P.; Kildishev, A.V.; Ni, X.; Chettiar, U.K.; Yuan, H.-K.; Shalaev, V.M. Loss-free and active optical negative-index metamaterials. *Nature* 2010, 466, 735.
11. Zhang, S.; Fan, W.J.; Panoiu, N.C.; Malloy, K.J.; Osgood, R.M.; Brueck, S.R.J. Experimental demonstration of near-infrared negative-index metamaterials. *Phys. Rev. Lett.* 2005, 95, 137404.
12. Ma, Q.; Shi, C.B.; Chen, T.Y.; Qi, M.Q.; Li, Y.B.; Cui, T.J. Broadband metamaterial lens antennas with special properties by controlling both refractive-index distribution and feed directivity. *J. Opt.* 2018, 20, 045101. (In English)
13. Kaina, N.; Lemoult, F.; Fink, M.; Lerosey, G. Negative refractive index and acoustic superlens from multiple scattering in single negative metamaterials. *Nature* 2015, 525, 77–81.
14. Kundtz, N.; Smith, D.R. Extreme-angle broadband metamaterial lens. *Nat. Mater.* 2010, 9, 129–132.

15. Pendry, J.B. Negative refraction makes a perfect lens. *Phys. Rev. Lett.* 2000, 85, 3966–3969.
16. Schurig, D.; Mock, J.; Justice, B.; Cummer, S.A.; Pendry, J.B.; Starr, A.; Smith, D.R. Metamaterial Electromagnetic Cloak at Microwave Frequencies. *Science* 2006, 314, 977–980.
17. Liang, Q.; Li, Z.; Jiang, Z.; Duan, Y.; Chen, T.; Li, D. A 3D-printed adaptive cloaking-illusion-integrated metasurface. *J. Mater. Chem. C* 2020, 8, 16018–16023.
18. Ergin, T.; Stenger, N.; Brenner, P.; Pendry, J.B.; Wegener, M. Three-dimensional invisibility cloak at optical wavelengths. *Science* 2010, 328, 337–339. (In English)
19. Hui, F.M.; Cui, T.J. Three-dimensional broadband ground-plane cloak made of metamaterials. *Nat. Commun.* 2010, 1, 21.
20. Ma, Q.; Mei, Z.L.; Zhu, S.K.; Jin, T.Y.; Cui, T.J. Experiments on active cloaking and illusion for Laplace equation. *Phys. Rev. Lett.* 2013, 111, 173901.
21. Yang, F.; Mei, Z.L.; Jin, T.Y.; Cui, T.J. dc Electric Invisibility Cloak. *Phys. Rev. Lett.* 2012, 109, 053902.
22. Xiang, N.; Cheng, Q.; Chen, H.B.; Zhao, J.; Jiang, W.X.; Ma, H.F.; Cui, T.J. Bifunctional metasurface for electromagnetic cloaking and illusion. *Appl. Phys. Express* 2015, 8, 092601.
23. Ma, Q.; Yang, F.; Jin, T.Y.; Mei, Z.L.; Cui, T.J. Open active cloaking and illusion devices for the Laplace equation. *J. Opt.* 2016, 18, 044004. (In English)
24. Han, T.; Bai, X.; Gao, D.; Thong, J.T.L.; Li, B.; Qiu, C.-W. Experimental Demonstration of a Bilayer Thermal Cloak. *Phys. Rev. Lett.* 2014, 112, 054302.
25. Jha, P.K.; Ni, X.; Wu, C.; Wang, Y.; Zhang, X. Metasurface-Enabled Remote Quantum Interference. *Phys. Rev. Lett.* 2015, 115, 025501.
26. Cui, T.-J.; Liu, S.; Li, L.-L. Information entropy of coding metasurface. *Light-Sci. Appl.* 2016, 5, e16172.
27. Aristov, A.I.; Zywiets, U.; Evlyukhin, A.B.; Reinhardt, C.; Chichkov, B.N.; Kabashin, A.V. Laser-ablative engineering of phase singularities in plasmonic metamaterial arrays for biosensing applications. *Appl. Phys. Lett.* 2014, 104, 071101.
28. Xu, W.; Huang, Y.; Zhou, R.; Wang, Q.; Yin, J.; Kono, J.; Ying, Y. Metamaterial-Free Flexible Graphene-Enabled Terahertz Sensors for Pesticide Detection at Bio-Interface. *ACS Appl. Mater. Interfaces* 2020, 12, 44281–44287.
29. Shin, D.; Urzhumov, Y.; Jung, Y.; Kang, G.; Baek, S.; Choi, M.; Smith, D.R. Broadband electromagnetic cloaking with smart metamaterials. *Nat. Commun.* 2012, 3, 1213.
30. Fang, N.; Lee, H.; Sun, C.; Zhang, X. Sub-diffraction-limited optical imaging with a silver superlens. *Science* 2005, 308, 534–537. (In English)
31. Leonhardt, U. Perfect imaging without negative refraction. *New J. Phys.* 2009, 11, 093040. (In English)
32. Huang, L.; Chen, X.; Mühlenbernd, H.; Zhang, H.; Chen, S.; Bai, B.; Qiu, C.-W. Three-dimensional optical holography using a plasmonic metasurface. *Nat. Commun.* 2013, 4, 2808.
33. Ding, X.; Wang, Z.; Hu, G.; Liu, J.; Zhang, K.; Li, H.; Ratni, B.; Burokur, S.N.; Wu, Q.; Tan, J.; et al. Metasurface holographic image projection based on mathematical properties of Fourier transform. *Photonix* 2020, 1, 16.
34. Wang, D.; Liu, C.; Shen, C.; Xing, Y.; Wang, Q.-H. Holographic capture and projection system of real object based on tunable zoom lens. *Photonix* 2020, 1, 6.
35. Zhao, R.; Huang, L.; Wang, Y. Recent advances in multi-dimensional metasurfaces holographic technologies. *Photonix* 2020, 1, 20.
36. Zou, X.; Zhen, G.; Yuan, Q.; Zang, W.; Zhu, S. Imaging based on metalenses. *Photonix* 2020, 1, 2.
37. Cheng, Q.; Cui, T.J.; Jiang, W.X.; Cai, B.G. An omnidirectional electromagnetic absorber made of metamaterials. *New J. Phys.* 2010, 12, 063006. (In English)
38. Ma, H.F.; Cui, T.J. Three-dimensional broadband and broad-angle transformation-optics lens. *Nat. Commun.* 2010, 1, 124.
39. Mei, Q.Q.; Wen, X.T.; Cui, T.J. A Broadband Bessel Beam Launcher Using Metamaterial Lens. *Sci. Rep.* 2015, 5, 11732.
40. Chen, X.; Ma, H.F.; Zou, X.Y.; Jiang, W.X.; Cui, T.J. Three-dimensional broadband and high-directivity lens antenna made of metamaterials. *J. Appl. Phys.* 2011, 110, 044904. (In English)
41. Jiang, W.X.; Qiu, C.W.; Han, T.C.; Cheng, Q.; Ma, H.F.; Zhang, S.; Cui, T.J. Broadband all-dielectric magnifying lens for far-field high-resolution imaging. *Adv. Mater.* 2013, 25, 6963–6968.

42. Huang, S.-T.; Hsu, S.-F.; Tang, K.-Y.; Yen, T.-J.; Yao, D.-J. Application of a Terahertz System Combined with an X-Shaped Metamaterial Microfluidic Cartridge. *Micromachines* 2020, 11, 74.
43. Lee, W.; Jung, Y.; Jung, H.; Seo, C.; Choo, H.; Lee, H. Wireless-Powered Chemical Sensor by 2.4 GHz Wi-Fi Energy-Harvesting Metamaterial. *Micromachines* 2019, 10, 12.
44. Sievenpiper, D.; Zhang, L.J.; Broas, R.F.J.; Alexopolous, N.G.; Yablonovitch, E. High-impedance electromagnetic surfaces with a forbidden frequency band. *IEEE Trans. Microw. Theory Tech.* 1999, 47, 2059–2074.
45. Yu, N.F.; Genevet, P.; Kats, M.A.; Aieta, F.; Tetienne, J.-P.; Capasso, F.; Gaburro, Z. Light Propagation with Phase Discontinuities: Generalized Laws of Reflection and Refraction. *Science* 2011, 334, 333–337. (In English)
46. Schlickriede, C.; Kruk, S.S.; Wang, L.; Sain, B.; Kivshar, Y.; Zentgraf, T. Nonlinear Imaging with All-Dielectric Metasurfaces. *Nano Lett.* 2020, 20, 4370–4376.
47. Shen, B.L.; Liu, L.; Li, Y.; Ren, S.; Yan, J.; Hu, R.; Qu, J. Nonlinear Spectral-Imaging Study of Second- and Third-Harmonic Enhancements by Surface-Lattice Resonances. *Adv. Opt. Mater.* 2020, 8, 1901981.
48. Wan, W.; Gao, J.; Yang, X. Metasurface holograms for holographic imaging. *Adv. Opt. Mater.* 2017, 5, 1700541.
49. Xin, M.; Xie, R.; Zhai, G.; Gao, J.; Zhang, D.; Wang, X.; Ding, J. Full control of dual-band vortex beams using a high-efficiency single-layer bi-spectral 2-bit coding metasurface. *Opt. Express* 2020, 28, 17374–17383.
50. Zheng, Q.; Li, Y.; Han, Y.; Feng, M.; Pang, Y.; Wang, J.; Zhang, J. Efficient orbital angular momentum vortex beam generation by generalized coding metasurface. *Appl. Phys. A-Mater. Sci. Process.* 2019, 125, 136. (In English)
51. Chen, Y.; Shen, W.G.; Li, Z.M.; Hu, C.Q.; Jin, X.M. Underwater transmission of high-dimensional twisted photons over 55 meters. *Photonix* 2020, 1, 5.
52. Fu, S.; Zhai, Y.; Zhang, J.; Liu, X.; Gao, C. Universal orbital angular momentum spectrum analyzer for beams. *Photonix* 2020, 1, 19.
53. Qiao, Z.; Wan, Z.; Xie, G.; Wang, J.; Qian, L.; Fan, D. Multi-vortex laser enabling spatial and temporal encoding. *Photonix* 2020, 1, 13.
54. Ni, X.; Wong, Z.J.; Mrejen, M.; Wang, Y.; Zhang, X. An ultrathin invisibility skin cloak for visible light. *Science* 2015, 349, 1310–1314.
55. Toan, D.P.; Le, K.Q.; Lee, J.-H.; Khang, N.T. A Designed Broadband Absorber Based on ENZ Mode Incorporating Plasmonic Metasurfaces. *Micromachines* 2019, 10, 673.
56. Chen, L.; Ruan, Y.; Luo, S.S.; Ye, F.J.; Cui, H.Y. Optically Transparent Metasurface Absorber Based on Reconfigurable and Flexible Indium Tin Oxide Film. *Micromachines* 2020, 11, 1032.
57. Baier, M.; Grote, N.; Moehrl, M.; Sigmund, A. Integrated transmitter devices on InP exploiting electro-absorption modulation. *Photonix* 2020, 1, 4.
58. Guan, C.; Wang, Z.; Ding, X.; Zhang, K.; Ratni, B.; Burokur, S.N.; Wu, Q. Coding Huygens' metasurface for enhanced quality holographic imaging. *Opt. Express* 2019, 27, 7108–7119.
59. Pfeiffer, C.; Grbic, A. Metamaterial Huygens' Surfaces: Tailoring Wave Fronts with Reflectionless Sheets. *Phys. Rev. Lett.* 2013, 110, 197401.
60. Luo, Z.; Chen, M.Z.; Wang, Z.X.; Zhou, L.; Li, Y.B.; Cheng, Q.; Cui, T.J. Digital Nonlinear Metasurface with Customizable Nonreciprocity. *Adv. Funct. Mater.* 2019, 29, 1906635. (In English)
61. Ma, Q.; Chen, L.; Jing, H.B.; Hong, Q.R.; Cui, H.Y.; Liu, Y.; Cui, T.J. Controllable and Programmable Nonreciprocity Based on Detachable Digital Coding Metasurface. *Adv. Opt. Mater.* 2019, 7, 1901285. (In English)
62. Wang, X.; Zhang, G.; Li, H.; Zhou, J. Magnetically tunable Fano resonance with enhanced nonreciprocity in a ferrite-dielectric metamolecule. *Appl. Phys. Lett.* 2018, 112, 174103.
63. Bang, S.; Kim, J.; Yoon, G.; Tanaka, T.; Rho, J. Recent Advances in Tunable and Reconfigurable Metamaterials. *Micromachines* 2018, 9, 560.
64. Gil, I.; Bonache, J.; Garcia-Garcia, J.; Martin, F. Tunable metamaterial transmission lines based on varactor-loaded split-ring resonators. *IEEE Trans. Microw. Theory Tech.* 2006, 54, 2665–2674.
65. Zhang, F.; Zhao, Q.; Kang, L.; Gaillot, D.P.; Zhao, X.; Zhou, J. Magnetic control of negative permeability metamaterials based on liquid crystals. *Appl. Phys.* 2008, 92, 225–227.
66. Zhao, Q.; Kang, L.; Du, B.; Li, B.; Zhou, J.; Tang, H.; Zhang, B. Electrically tunable negative permeability metamaterials based on nematic liquid crystals. *Appl. Phys. Lett.* 2007, 90, 011112.

67. Sun, S.; Jiang, W.; Gong, S.; Tao, H. Reconfigurable Linear-to-Linear Polarization Conversion Metasurface Based on PIN Diodes. *IEEE Antennas Wirel. Propag. Lett.* 2018, 17, 1722–1726.
68. Farzami, F.; Khaledian, S.; Smida, B.; Erricolo, D. Reconfigurable Linear/Circular Polarization Rectangular Waveguide Filter. *IEEE Trans. Antennas Propag.* 2017, 66, 9–15.
69. Clemente, A.; Dussopt, L.; Sauleau, R.; Potier, P.; Pouliguen, P. 1-Bit Reconfigurable Unit Cell Based on PIN Diodes for Transmit-Array Applications in X-Band. *IEEE Trans. Antennas Propag.* 2012, 60, 2260–2269.
70. Xu, W.; Sonkusale, S. Microwave diode switchable metamaterial reflector/absorber. *Appl. Phys. Lett.* 2013, 103, OP98–OP120.
71. Gupta, B.; Pandey, S.; Nahata, A.; Zhang, T.; Nahata, A. Bistable Physical Geometries for Terahertz Plasmonic Structures Using Shape Memory Alloys. *Adv. Opt. Mater.* 2017, 5, 1601008.
72. Chen, Z.; Rahmani, M.; Gong, Y.; Chong, C.T.; Hong, M. Realization of Variable Three-Dimensional Terahertz Metamaterial Tubes for Passive Resonance Tunability. *Adv. Mater.* 2012, 24, OP143–OP147.
73. Ee, H.S.; Agarwal, R. Tunable Metasurface and Flat Optical Zoom Lens on a Stretchable Substrate. *Nano Lett.* 2016, 16, 2818–2823.
74. Huang, Y.W.; Lee, H.W.; Sokhoyan, R.; Pala, R.A.; Thyagarajan, K.; Han, S. Gate-Tunable Conducting Oxide Metasurfaces. *Nano Lett.* 2016, 16, 5319.
75. Ou, J.Y.; Plum, E.; Zhang, J.; Zheludev, N.I. An electromechanically reconfigurable plasmonic metamaterial operating in the near-infrared. *Nat. Nanotechnol.* 2013, 8, 252–255.
76. Xu, J.; Wang, J.; Yang, R.; Tian, J.; Chen, X.; Zhang, W. Frequency-tunable metamaterial absorber with three bands. *Opt. Int. J. Light Electron Opt.* 2018, 172, 1057–1063.
77. Zhang, X.G.; Tang, W.X.; Jiang, W.X.; Bai, G.D.; Tang, J.; Bai, L.; Cui, T.J. Light-Controllable Digital Coding Metasurfaces. *Adv. Sci.* 2018, 5, 1801028.
78. Xu, W.; Xie, L.; Ying, Y. Mechanisms and applications of terahertz metamaterial sensing: A review. *Nanoscale* 2017, 9, 13864–13878.
79. Grady, N.K.; Heyes, J.E.; Chowdhury, D.R.; Zeng, Y.; Reiten, M.T.; Azad, A.K.; Chen, H.-T. Terahertz Metamaterials for Linear Polarization Conversion and Anomalous Refraction. *Science* 2013, 340, 1304–1307.
80. Ni, X.; Kildishev, A.V.; Shalaev, V.M. Metasurface holograms for visible light. *Nat. Commun.* 2013, 4, 2807.
81. Yao, Y.; Shankar, R.; Kats, M.A.; Song, Y.; Kong, J.; Loncar, M.; Capasso, F. Electrically Tunable Metasurface Perfect Absorbers for Ultrathin Mid-Infrared Optical Modulators. *Nano Lett.* 2014, 14, 6526–6532.
82. della Giovampaola, C.; Engheta, N. Digital metamaterials. *Nat. Mater.* 2014, 13, 1115.
83. Cui, T.J.; Qi, M.Q.; Wan, X.; Zhao, J.; Cheng, Q. Coding metamaterials, digital metamaterials and programmable metamaterials. *Light-Sci. Appl.* 2014, 3, e218. (In English)
84. Cui, T.J.; Li, L.; Liu, S.; Ma, Q.; Zhang, L.; Wan, X.; Cheng, Q. Information Metamaterial Systems. *iScience* 2020, 23, 101403.
85. Xiao, Q.; Ma, Q.; Yan, T.; Wu, L.W.; Liu, C.; Wang, Z.X.; Cui, T.J. Orbital-Angular-Momentum-Encrypted Holography Based on Coding Information Metasurface. *Adv. Opt. Mater.* 2021, 9, 2002155.
86. Yan, T.; Ma, Q.; Sun, S.; Xiao, Q.; Shahid, I.; Gao, X.; Cui, T.J. Polarization Multiplexing Hologram Realized by Anisotropic Digital Metasurface. *Adv. Theory Simul.* 2021, 4, 2100046.
87. Zhang, L.; Wu, R.Y.; Bai, G.D.; Wu, H.T.; Ma, Q.; Chen, X.Q.; Cui, T.J. Transmission-Reflection-Integrated Multifunctional Coding Metasurface for Full-Space Controls of Electromagnetic Waves. *Adv. Funct. Mater.* 2018, 28, 1802205. (In English)
88. Bai, G.D.; Ma, Q.; Cao, W.K.; Li, R.Q.; Jing, H.B.; Mu, J. Manipulation of Electromagnetic and Acoustic Wave Behaviors via Shared Digital Coding Metallic Metasurfaces. *Adv. Intell. Syst.* 2019, 1, 1900038.
89. Jing, H.B.; Ma, Q.; Bai, G.D.; Bao, L.; Luo, J.; Cui, T.J. Optically transparent coding metasurfaces based on indium tin oxide films. *J. Appl. Phys.* 2018, 124, 023102.
90. Luo, J.; Ma, Q.; Jing, H.; Bai, G.; Wu, R.; Bao, L.; Cui, T.J. 2-bit amplitude-modulated coding metasurfaces based on indium tin oxide films. *J. Appl. Phys.* 2019, 126, 113102.
91. Ma, Q.; Shi, C.B.; Bai, G.D.; Chen, T.Y.; Noor, A.; Cui, T.J. Beam-Editing Coding Metasurfaces Based on Polarization Bit and Orbital-Angular-Momentum-Mode Bit. *Adv. Opt. Mater.* 2017, 5, 1700548. (In English)

92. Hong, Q.R.; Ma, Q.; Gao, X.X.; Liu, C.; Xiao, Q.; Iqbal, S.; Cui, T.J. Programmable Amplitude-Coding Metasurface with Multifrequency Modulations. *Adv. Intell. Syst.* 2021, 2000260.
93. Bai, G.D.; Ma, Q.; Iqbal, S.; Bao, L.; Jing, H.B.; Zhang, L.; Cui, T.J. Multitasking Shared Aperture Enabled with Multiband Digital Coding Metasurface. *Adv. Opt. Mater.* 2018, 6, 1800657. (In English)
94. Ma, Q.; Cui, T.J. Information Metamaterials: Bridging the physical world and digital world. *PhotoniX* 2020, 1, 1.
95. Bao, L.; Ma, Q.; Bai, G.D.; Jing, H.B.; Wu, R.Y.; Fu, X.; Cui, T.J. Design of digital coding metasurfaces with independent controls of phase and amplitude responses. *Appl. Phys. Lett.* 2018, 113, 063502. (In English)
96. Bai, G.D.; Ma, Q.; Li, R.Q.; Mu, J.; Cui, T.J. Spin-Symmetry Breaking Through Metasurface Geometric Phases. *Phys. Rev. Appl.* 2019, 12, 044042.
97. Chen, L.; Ma, Q.; Jing, H.B.; Cui, H.Y.; Liu, Y.; Cui, T.J. Space-Energy Digital-Coding Metasurface Based on an Active Amplifier. *Phys. Rev. Appl.* 2019, 11, 054051. (In English)
98. Chen, L.; Ma, Q.; Nie, Q.F.; Hong, Q.R.; Cui, H.Y.; Ruan, Y.; Cui, T.J. Dual-polarization programmable metasurface modulator for near-field information encoding and transmission. *Photonics Res.* 2021, 9, 116–124.
99. Ma, Q.; Hong, Q.R.; Bai, G.D.; Jing, H.B.; Cui, T.J. Editing Arbitrarily Linear Polarizations Using Programmable Metasurface. *Phys. Rev. Appl.* 2020, 13, 021003. (In English)
100. Ma, Q.; Bai, G.D.; Jing, H.B.; Yang, C.; Li, L.; Cui, T.J. Smart metasurface with self-adaptively reprogrammable functions. *Light-Sci. Appl.* 2019, 8, 98.
101. Ma, Q.; Hong, Q.R.; Gao, X.X.; Jing, H.B.; Liu, C.; Bai, G.D.; Cui, T.J. Smart sensing metasurface with self-defined functions in dual polarizations. *Nanophotonics* 2020, 9, 3271–3278. (In English)
102. Li, L.; Shuang, Y.; Ma, Q.; Li, H.; Zhao, H.; Wei, M.; Cui, T.J. Intelligent metasurface imager and recognizer. *Light Sci. Appl.* 2019, 8, 1–9.
103. Goi, E.; Zhang, Q.; Chen, X.; Luan, H.; Gu, M. Perspective on photonic memristive neuromorphic computing. *PhotoniX* 2020, 1, 3.

Retrieved from <https://encyclopedia.pub/entry/history/show/32830>